Numerical Simulation of Trapped Field and Temperature Rise in MgB_2 Bulks Magnetized by Pulsed Field

Hiroyuki Fujishiro, Tomoyuki Naito, Mitsuru Oyama, Takahiro Arayashiki, Takuya Tamura, Tomohisa Sasaki, and Giovanni Giunchi

***Abstract*—Pulsed field magnetization (PFM) was performed for the MgB_2 bulk 30 mm in diameter and the applied pulsed-field dependence of the trapped field B_T^C, temperature rise ΔT and time dependence of the local field $B_L^C(t)$ were measured on the bulk. $B_T^C = 0.71$ T was achieved at 14 K after applying the pulsed field of $B_{ex} = 1.55$ T, where ΔT of about 10 K was observed. Numerical simulation of PFM was also performed and B_T^C, ΔT and $B_L^C(t)$ were simulated. The results of the simulation reproduced the experimental ones qualitatively. The flux dynamics and the heat generation in the MgB_2 bulk during PFM were in clear contrast with those in REBaCuO bulks because of a small specific heat, large thermal conductivity, and narrow temperature margin against the transition temperature T_c.**

***Index Terms*—MgB_2 bulk, numerical simulation, pulsed-field magnetization, trapped field.**

I. Introduction

THE superconducting bulk magnet using a REBaCuO (RE: rare earth element or Y) is one of the typical models for practical applications such as sputtering cathodes, magnetic separation and drug delivery systems (DDSs) [1], which produces tesla-order quasi-permanent magnets. However, it is difficult to fabricate a large single-domain bulk over 100 mm in diameter. MgB_2 bulk has also a promising potential as a quasi-permanent magnet, which has several attractive natures for bulk magnet, such as low-cost, light-weight and homogeneous trapped field distribution, which are in clear contrast with the REBaCuO bulk magnet. The problem of weak-links at grain boundaries can be ignored in the MgB_2 polycrystalline bulk due to their long coherence length, ξ [2]. These characteristics enable us to realize the better and larger polycrystalline MgB_2 bulk magnets below the transition temperature $T_c = 39$ K. Several groups have already reported the trapped field on the MgB_2 bulk by the field-cooled magnetization (FCM), and attained the trapped field over 1.5 T at low temperatures [3]–[5]. MgB_2 magnets are expected to be applicable in magnetically levitated trains (MAGLEVs) and wind power generators using liquid H_2 or cryocooler cooling.

Pulsed-field magnetization (PFM) has also been investigated to magnetize the bulk superconductors because of an inexpensive and mobile experimental setup with no need for a superconducting coil magnet. However, for the REBaCuO bulks, the trapped field B_z achievable by PFM is nonetheless lower than that achievable by FCM because of the large temperature rise caused by the dynamical motion of the magnetic flux. Several approaches have been performed and succeeded in enhancing B_z using the multi-pulse techniques [6], [7]. We have experimentally examined the trapped field B_z on the surface of cryocooled REBaCuO bulks during PFM for various starting temperatures T_s and applied fields B_{ex} [8]. To enhance B_z, the reduction in temperature rise and the lowering of T_s are effective. Considering the obtained experimental results, we proposed a new PFM technique named a modified multi-pulse technique with stepwise cooling (MMPSC) and successfully realized a highest field trap of $B_z = 5.20$ T on a GdBaCuO bulk with 45 mm in diameter at 30 K [9], which is a record-high value magnetized by PFM to date.

In the previous paper, we have performed the PFM to a large MgB_2 bulk 50 mm in diameter fabricated by a reactive liquid Mg infiltration (Mg-RLI) method [10], in which the trapped field of $B_z = 0.47$ T was achieved at $T_s = 23$ K. However, the trapped field profiles were inhomogeneous because of the inhomogeneous J_c distribution in the bulk. It is necessary to investigate the flux dynamics and heat generation using a homogeneous MgB_2 bulk experimentally and numerically.

In this study, we applied the PFM technique to the homogeneous MgB_2 bulk fabricated by a capsule method [11] and analyzed the PFM process using the numerical simulation. In the PFM for the MgB_2 bulk, flux dynamics and heat generation are supposed to be a clear contrast with those in the REBaCuO bulk because of the small specific heat, large thermal conductivity, and narrow temperature margin against T_c. Using the simulation, a characteristic aspect in MgB_2 during PFM was discussed.

II. Experimental Procedure

MgB_2 bulk was fabricated by the *in-situ* capsule method [11]. Raw powders of Mg (99% in purity) and amorphous B

Manuscript received October 3, 2012; accepted December 27, 2012. Date of publication January 4, 2013; date of current version April 10, 2013. This work supported in part by a Grant-in-Aid for Scientific Research (No. 23560002) from the Ministry of Education, Culture, Sports, Science and Technology, Japan, Japan Science and Technology Agency under a Research for Promoting Technological Seeds 2009 (02-051) and an Adaptable and Seamless Technology Transfer Program through target-driven R&D for an Exploratory Research of FS stage (AS232Z02579B).

H. Fujishiro, T. Naito, M. Oyama, T. Arayashiki, T. Tamura, and T. Sasaki are with the Faculty of Engineering, Iwate University, Morioka 020-8551, Japan (e-mail: fujishiro@iwate-u.ac.jp).

G. Giunchi is with EDISON S.p.A., R&D Division, 20121 Milano, Italy (e-mail: giovanni.giunchi@edison.it).

Color versions of one or more of the figures in this paper are available online at http://ieeexplore.ieee.org.

Digital Object Identifier 10.1109/TASC.2012.2237224

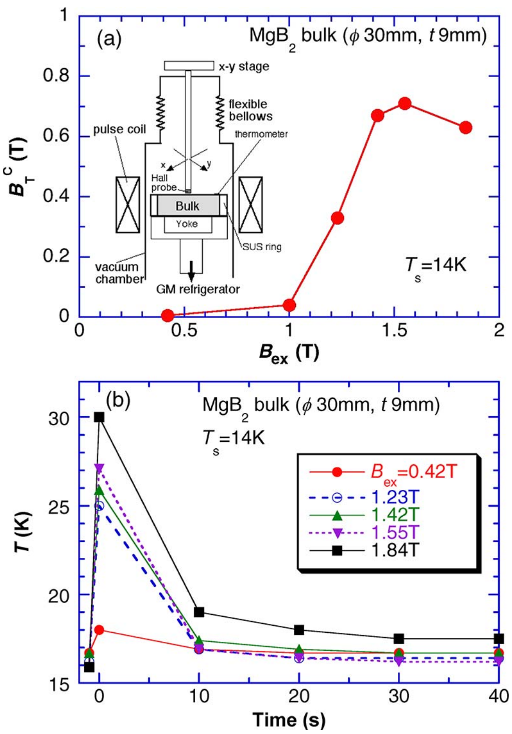

Fig. 1. (a) Experimental results of the trapped field $B_{\mathrm{T}}^{\mathrm{C}}$ at the center of the MgB_2 bulk surface as a function of applied pulsed field B_{ex} at $T_{\mathrm{s}} = 14$ K. Inset shows the experimental setup. (b) Time dependences of the temperature $T(t)$ on the bulk surface for each applied field B_{ex}

(99% in purity) were weighted with 1.1: 2.0 in molar ratio, ground and was pressed into pellet 30 mm in diameter and 9 mm in thickness under uniaxial pressure of 12 MPa in air. The precursor pellet sealed in the stainless steel (SUS304) capsule by Ar gas was sintered at 800 °C for 6 h in a box furnace and then cooled to room temperature.

The MgB_2 bulk was tightly anchored onto the cold stage of a Gifford-McMahon (GM) cycle helium refrigerator as shown in the inset of Fig. 1(a). The initial temperature T_{s} of the bulk was 14 K. The magnetizing solenoid coil (99 mm I.D., 121 mm O.D., and 50 mm height), which was dipped in liquid nitrogen, was placed outside the vacuum chamber. A magnetic pulse B_{ex} up to 1.85 T with a rise time of 0.01 s was applied by flowing the pulsed current to the coil. The time evolutions of the local field $B_{\mathrm{L}}^{\mathrm{C}}(t)$ and the subsequent trapped field $B_{\mathrm{T}}^{\mathrm{C}}$ at the bulk center were monitored by the Hall sensor (BHT 921; F W Bell), which was adhered at the center of the bulk surface. Two-dimensional trapped field profiles of B_{z} (1 mm) were mapped on the bulk with 1 mm above the bulk surface, stepwise with a pitch of 1 mm by scanning the axial-type Hall sensor (BHA 921; F W Bell) using an $x - y$ stage controller. During PFM, the time dependence of temperature $T(t)$ was also measured at the bulk surface of using the thermometers (Cernox; Lakeshore).

III. Model of Numerical Simulation for PFM

Based on the experimental setup, the framework of the numerical simulation was constructed using the axi-symmetric coordinate. The detailed procedure of the simulation was described elsewhere [12]. The sizes of the bulk and the magnetizing solenoid coil were the same as those of the experimental condition. Physical phenomena during PFM were described using electromagnetic and thermal fields, which were taken from [13]. The power-n model $(10 \leq n \leq 100)$ was supposed to describe the nonlinear $E - J$ characteristic in the bulk. The temperature and magnetic field dependences of the critical current density $J_{\mathrm{c}}(T, B)$ were described as,

$$J_c(T,B) = J_{c0}\frac{B_0}{|B|+B_0} = \alpha\left\{1-\left(\frac{T}{T_c}\right)^2\right\}^{\frac{3}{2}}\frac{B_0}{|B|+B_0} \quad (1)$$

where $T_{\mathrm{c}}(= 39\ \mathrm{K})$ is the critical temperature at $B = 0$, and $B_0(= 1.3\ \mathrm{T})$ is constant. In (1), α shows the strength of J_{c0} and was changed from 2.0×10^8 and 1.0×10^9 A/m^2, which represents $J_{\mathrm{c0}} = 1.6 \times 10^8$ and 8.1×10^8 A/m^2 at 14 K, respectively. Although the thermal conductivity κ and the specific heat C values of the MgB_2 bulk were steeply temperature-dependent [14], [15], constant values of $\kappa(= 80\ \mathrm{W\ m^{-1}\ K^{-1}})$ and $C(= 17.2\ \mathrm{J\ kg^{-1}\ K^{-1}})$ were adopted for simplicity. $\kappa(= 3.0\ \mathrm{W\ m^{-1}\ K^{-1}})$ and $C(= 30\ \mathrm{J\ kg^{-1}\ K^{-1}})$ of the SUS304 capsule, and the mass density ρ of MgB_2 (1.4 kg m^{-3}) and SUS304 (7.93 kg m^{-3}) were also supposed to be constant. Commercial software, Photo-Eddy, combined with Photo-Thermo (Photon Ltd.), was used for analyses of the magnetic field and temperature distribution in the MgB_2 bulk during PFM.

IV. Experimental Results

Fig. 1(a) shows the trapped field $B_{\mathrm{T}}^{\mathrm{C}}$ at the center of the bulk surface, as a function of the strength of the applied pulsed field B_{ex}. $B_{\mathrm{T}}^{\mathrm{C}}$ increases for $B_{\mathrm{ex}} > 1$ T, takes a maximum of $B_{\mathrm{T}}^{\mathrm{C}} = 0.71$ T at $B_{\mathrm{ex}} = 1.54$ T and then decreases with increasing B_{ex}. The $B_{\mathrm{T}}^{\mathrm{C}}$ vs B_{ex} curve is a typical one for PFM in REBCO bulks [8]. Fig. 1(b) shows the time dependence of the temperature change on the bulk surface for each applied field B_{ex}. The temperature increases abruptly just after the pulse application and sharply decreases with increasing time. The magnitude of the maximum temperature rise increases with increasing B_{ex}. The sharp temperature change results from the small specific heat and high thermal conductivity of the bulk, compared with those for the REBaCuO bulk at operating temperatures.

Fig. 2 presents the trapped field profiles B_{z} (1 mm) for various applied pulsed fields B_{ex}. For $B_{\mathrm{ex}} = 1.04$ T as shown in Fig. 2(a), the magnetic flux was trapped at the right lower region of the bulk, where the critical current density J_{c} seems to be relatively lower. For $B_{\mathrm{ex}} = 1.23$ T as shown in Fig. 2(b), the magnetic flux was also trapped at the left upper region of the bulk. For $B_{\mathrm{ex}} = 1.42$ T and 1.54 T as shown in Fig. 2(c) and (d), the trapped field profiles are nearly the conical one which look like nearly homogeneous, compared with those for the REBaCuO bulks [8]. Because the MgB_2 bulk was polycrystal and was fabricated by the *in-situ* sintering method. On the other hand, the REBaCuO bulk was fabricated by the melt-growth, in which the four-fold growth sector boundaries (GSBs) with higher J_{c} exist.

Fig. 3 shows an example of the time dependence of the local field $B_{\mathrm{L}}^{\mathrm{C}}(t)$ and pulsed field $B_{\mathrm{ex}}(t)$ at $B_{\mathrm{ex}} = 1.54$ T. $B_{\mathrm{L}}^{\mathrm{C}}(t)$ starts to increase with a slight time delay, takes a maximum

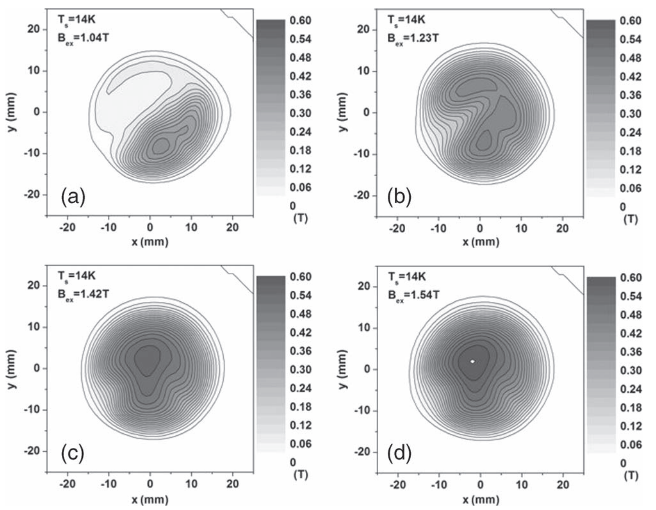

Fig. 2. Trapped field profiles B_z on the MgB_2 bulk 1 mm above the bulk surface at $T_s = 14$ K at (a) $B_{ex} = 1.04$ T, (b) 1.23 T, (c) 1.42 T, and (d) 1.54 T.

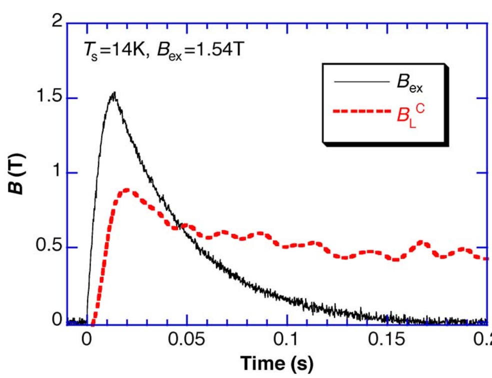

Fig. 3. Time dependences of the local field $B_L^C(t)$ and the applied pulsed field $B_{ex}(t)$ for $B_{ex} = 1.54$ T.

at 0.015 s and then decreases to a final value due to the flux flow. The maximum $B_L^C(t)$ increased with increasing B_{ex} and is smaller than that of $B_{ex}(t)$ because of the shielding effect.

FCM was also performed for the same bulk. The highest B_T^C value was 1.50 T at 16 K and decreased with increasing temperature. The trapped field B_T^{FCM} (4 mm) at $T_s = 28$ K was 0.32 T and the trapped field profile was conical, which suggests that the J_c distribution in the bulk is nearly homogeneous also from the profile by FCM.

V. Results of Numerical Simulation

Fig. 4(a) depicts the results of simulation for the trapped field B_T^C at the center of the bulk surface, as a function of the applied field B_{ex} for various J_{c0} values ($n = 50$). In all the cases, B_T^C starts to increase, takes a maximum, and then decreases with a further increase in B_{ex}. The critical applied field B_{ex}^C, at which the magnetic flux starts to trap at the bulk center, increases with increasing J_{c0}. Fig. 4(b) shows the results of simulation for the B_T^C as a function of the B_{ex} for various n-values ($J_{c0} = 4.1 \times 10^8$ A/m^2). The $B_T^C - B_{ex}$ curve shifts to the low B_{ex} side with increasing n-value, but then the shift between $n = 50$ and 100 was relatively small. These results suggest that the simulation using the conditions ($J_{c0} = 4.1 \times 10^8$ A/m^2 and $n = 50$) well

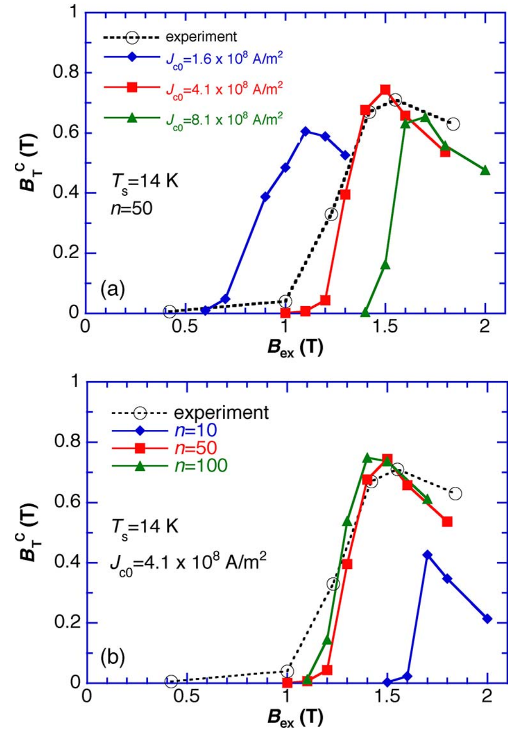

Fig. 4. Results of the simulation of the (a) trapped field B_T^C for various J_{c0} values and (b) B_T^C for various n-values, as a function of the applied field B_{ex} The experimental results were reproduced by the simulation using the parameters of $J_{c0} = 4.1 \times 10^8$ A/m^2 and $n = 50$.

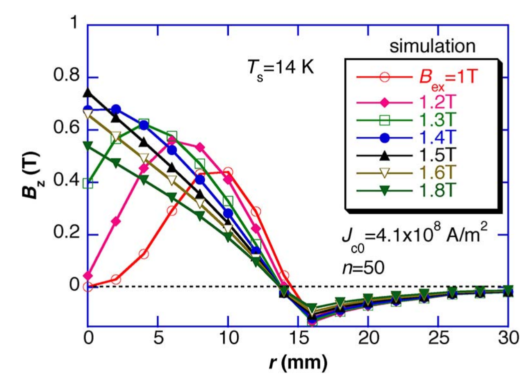

Fig. 5. Results of the simulation of the radial dependence of the trapped field $B_z(r)$ at $T_s = 14$ K for various B_{ex} ($J_{c0} = 4.1 \times 10^8$ A/m^2 and $n = 50$).

reproduces the experimental results. Thereafter, we discuss the flux dynamics and heat generation in the bulk during PFM using these conditions.

Fig. 5 presents the radial dependence of the trapped field profile $B_z(r)$ on the bulk for various B_{ex}. The positions of $r = 0$ and 15 mm are, respectively, the center and the edge of the bulk surface. The $B_z(r)$ profile changes from concave for a lower B_{ex} to convex for a higher B_{ex} and then the $B_z(r = 0)$ value decreases with a further increase in B_{ex}.

Fig. 6 shows the time dependences of the local fields $B_T^C(t)$ at the center of the bulk surface for various B_{ex}. The time dependence of the magnetic pulse $B_{ex}(t)$ at 1.5 T is also shown. The local field $B_L^C(t)$ starts to increase rapidly with a time lag and then decreases.

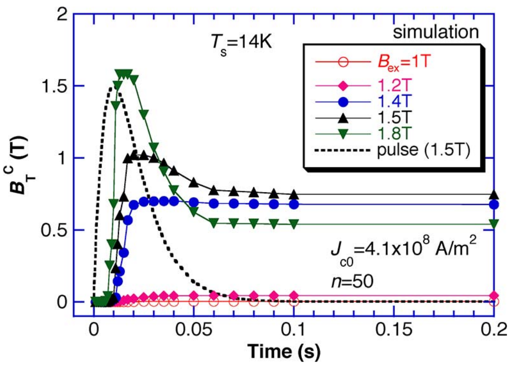

Fig. 6. Results of the simulation of the time dependence of the local field $B_L^C(t)$ at the center of the bulk surface at $T_s = 14$ K for various applied fields B_{ex} ($J_{c0} = 4.1 \times 10^8$ A/m^2 and $n = 50$).

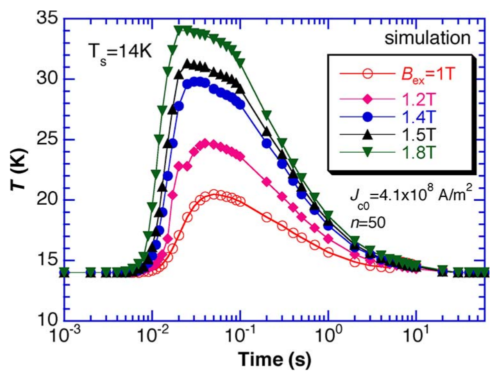

Fig. 7. Results of the simulation of the time dependence of the temperature $T(t)$ at the center of the bulk surface at $T_s = 14$ K for various applied fields B_{ex} ($J_{c0} = 4.1 \times 10^8$ A/m^2 and $n = 50$).

Fig. 7 shows results of the simulation for the time dependences of temperature $T(t)$ at the center of the bulk surface for various B_{ex}. $T(t)$ starts to rise rapidly at $t = 0.01$ s, at which $B_{ex}(t)$ takes a maximum. $T(t)$ takes a maximum at $t = 0.02$–0.05 s, which becomes shorter with increasing B_{ex} and then decreases. In Fig. 6, a steep decrease in $B_L^C(t)$ was seen for $B_{ex} = 1.8$ T, which results from the approach of the temperature to $T_c = 39$ K because of the large temperature rise. For higher B_{ex}, the temperature at the bulk periphery exceeded T_c and most of the trapped flux escaped from the bulk.

The results of the simulation for the MgB_2 bulk were in clear contrast with those for REBaCuO bulks [8]; the trapped field B_T^C was a broad applied field dependence and $T(t)$ took a maximum at 7 s. The differences come from the small specific heat, large thermal conductivity, and narrow temperature margin against the transition temperature T_c in the MgB_2 bulk. The use of numerical simulation can optimize the operating parameters for PFM to enhance the trapped field [12].

VI. Summary

Pulsed field magnetization (PFM) was performed for the homogeneous MgB_2 bulk 30 mm in diameter and the applied pulsed field dependence of the trapped field B_T^C, temperature rise and time dependence of the local field $B_L^C(t)$ were measured and simulated. Important results and conclusions obtained in this study are summarized as follows.

1) The maximum trapped field of $B_z = 0.71$ T was realized at the center of the bulk surface at $T_s = 14$ K after the magnetic pulse application of $B_{ex} = 1.55$ T.
2) The experimental results can be qualitatively reproduced by numerical simulation using electromagnetic and thermal fields.
3) The flux dynamics and the heat generation of the MgB_2 bulk during PFM were in clear contrast with those for REBaCuO bulks because of a small specific heat, large thermal conductivity, and narrow temperature margin against T_c in the MgB_2 bulk.

References

[1] M. Murakami, "Processing and applications of bulk RE–Ba–Cu–O superconductors," *Int. J. Appl. Ceram. Technol.*, vol. 4, pp. 225–241, 2007.

[2] M. Kambara, N. H. Babu, E. S. Sadki, J. R. Cooper, H. Minami, D. A. Cardwell, A. M. Campbell, and I. H. Inoue, "High intergranular critical currents in metallic MgB_2 superconductor," *Supercond. Sci. Technol.*, vol. 14, pp. L5–L8, 2001.

[3] R. V. Viznichenko, A. A. Kordyuk, G. Fuchs, K. Nenkov, K. H. Mnuller, T. A. Prikhna, and W. Gawalek, "Temperature dependence of the trapped magnetic field in MgB_2 bulk superconductors," *Appl. Phys. Lett.*, vol. 83, pp. 4360–4362, 2003.

[4] A. Yamamoto, H. Yumoto, J. Shimoyama, K. Kishio, A. Ishihara, and M. Tomita, "Development of MgB_2 bulk superconducting magnet," in *Proc. Abstract 23rd Int. Symp. Supercond.*, 2010, pp. 219–219.

[5] E. Perini, G. Giunchi, L. Saglietti, A. Albisetti, A. Matrone, and V. Cavaliere, "Magnetic field trapping in MgB_2 bulks and inserts," *IEEE Trans. Appl. Supercond.*, vol. 21, no. 3, pp. 2690–2693, Jun. 2011.

[6] Y. Yanagi, Y. Itoh, M. Yoshikawa, T. Oka, T. Hosokawa, H. Ishihara, H. Ikuta, and U. Mizutani, "Trapped field distribution on Sm-Ba-Cu-O bulk superconductor by pulsed-field magnetization," in *Advances in Superconductivity XII*. Tokyo, Japan: Springer-Verlag, 2000, pp. 470–473.

[7] M. Sander, U. Sutter, R. Koch, and M. Klaser, "Pulsed magnetization of HTS bulk parts at $T < 77$ K," *Supercond. Sci. Technol.*, vol. 13, pp. 841–845, 2000.

[8] H. Fujishiro, T. Hiyama, T. Miura, T. Naito, S. Nariki, N. Sakai, and I. Hirabayashi, "Pulsed field magnetization for GdBaCuO bulk with stronger pinning characteristics," *IEEE Trans. Appl. Supercond.*, vol. 19, no. 3, pp. 3545–3548, Jun. 2009.

[9] H. Fujishiro, T. Tateiwa, A. Fujiwara, T. Oka, and H. Hayashi, "Higher trapped field over 5 T on HTSC bulk by modified pulsed field magnetizing," *Phys. C*, vol. 445–448, pp. 334–338, 2006.

[10] H. Fujishiro, T. Tamura, T. Arayashiki, M. Oyama, T. Sasaki, T. Naito, G. Giunchi, and A. F. Albisetti, "Pulsed field magnetization of large MgB_2 bulk fabricated by reactive liquid mg infiltration," *Jpn. J. Appl. Phys.*, vol. 51, p. 103005, 2012.

[11] T. Naito, T. Sasaki, and H. Fujishiro, "Trapped magnetic field and vortex pinning properties of MgB_2 superconducting bulk fabricated by a capsule method," *Supercond. Sci. Technol.*, vol. 25, p. 095012, 2012.

[12] H. Fujishiro and T. Naito, "Simulation of temperature and magnetic field distribution in superconducting bulk during pulsed field magnetization," *Supercond. Sci. Technol.*, vol. 23, p. 105021, 2010.

[13] Y. Komi, M. Sekino, and H. Ohsaki, "Three-dimensional numerical analysis of magnetic and thermal fields during pulsed field magnetization of bulk superconductors with inhomogeneous superconducting properties," *Phys. C*, vol. 469, pp. 1262–1265, 2009.

[14] T. Cavallin, E. A. Young, C. Beduz, Y. Yang, and G. Giunchi, "Thermal conductivity of bulk MgB_2 produced by infiltration of different boron powders," *IEEE Trans. Appl. Supercond.*, vol. 17, no. 2, pp. 2770–2773, Jun. 2007.

[15] C. Walti, E. Felder, C. Degen, G. Wigger, R. Monnier, B. Delley, and H. R. Ott, "Strong electron-phonon coupling in superconducting MgB_2: A specific heat study," *Phys. Rev. B*, vol. 64, p. 172515, 2001.